NUMERO: **2557A** ANNO: 2023

A P P U N T I

STUDENTE: Vinci Flaminia

MATERIA: Nanosurfaces and Nanostructures, Exam Questions - Prof. Mandracci

Politecnico di Torino

Nanosurfaces and Nanostructures: from synthesis to application

Master's degree in Nanotechnologies for Smart and Integrated Systems
A.Y. 2022/2023 - Prof. Pietro Mandracci

Exam Questions

Part A, Part B and Part Prof. Cauda

Author: Flaminia Vinci

© Proprietà riservata dell'autore - Digitalizzazione e distribuzione a cura del CENTRO APPUNTI - Corso Luigi Einaudi, 55/B - Torino / Pagina 3 di 114

Contents

PART A. SURFACE INTERACTIONS

1.1 A1. Concerning the interaction between a surface and a gas or vapor, explain: - the main characteristics of physisorption and condensation; - the main characteristics of chemisorption; - the main characteristics of dissociative chemisorption.

Let's start by considering a surface exposed to a vapor or a gas. Vapor molecules impinge caothically on the material surface with a certain impingin rate R that quantifies the intensity of the interaction, since it is defined as the number of molecules impinging on a unit surface per unit time. ($[R] = [L^{-2}T^{-1}]$)

$$R = \frac{p}{\sqrt{2\pi m k_B T}} \tag{1.1}$$

Depending on the type of impinging molecules and on the chemical composition of the surface, they can be reflected back or may remain attached to the surface. The fraction of attached molecules is indicated by the sticking coefficient S:

$$S = N_{ads} \cdot N_{inc} = \frac{N_{ads}}{R \cdot A \cdot \Delta t} \tag{1.2}$$

Where N_{ads} is the number of molecules that will bond with the surface.
The molecules attach to the surface in several ways, for each of them there's a dfferent S.
The first mechanism theat we have studied is **Physisorption** also called Physical adsorption. The adsorption of a vapor or a gas usually starts with this.
The bond that is created between molecules and surface is of the electrostatic type and it is due to the close distance between them, so overall this interaction is quite weak. Indeed we deal about Van Der Waals forces between molecules.
Another characteristic of physisorption is that the electronic structure of the molecule remains unchanged, i.e. the chemical properties of the impinging molecule remain the same (same configuration of the electronic shell).
Last, the bond is so weak that ca be easily broken.
We can model a physisorbed atom (adatom) with a one-dimensional oscillator interacting with an

the motion, parallel to the surface plane, they can bond with other absorbed atoms/molecules or interact with surface defects.
The mean permanence time is the time after which, on average, the particle will desorb from the surface if it did not create a strong bond. The higher permanence time is of water (10^{-3}s).

For what regard the **Condensation process**, this is similar to physisorption, but now the atoms/-molecules are bonded to previously physisorbed layers one over the other. Usually, this occurs only at specific temperatures. The thicker are such layers, the less important becomes the interaction with the surface.

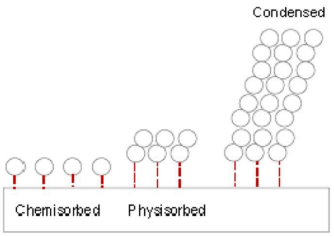

Typically $E_{cond} > E_{ads}$, which means that the energy required to remove the condensated layers is lower than the energy required to remove the adsorbed (physisorbed) atoms.

Regarding the **chemisorption** or **chemical adsorption**, the particle is able to create a strong bond with the surface,that is similar to the chemical bond between two atoms in a molecule. This is due to an interaction between the outer electron shells of the adsorbed molecule and the surface atoms. The result is a considerable change in the electronic structure of the impinging molecule [1]. Such strong bond cannot be broken easily at room temperature.
Also for chemisorption we can define a potential energy that chages with the distance from the surface. Also here, as the molecule approaches to the surface, the potential drops and when a minimum distance is overcame a repulsive force generates. The difference with physisorption is that the distance at which we have the minimum potential energy, i.e. z0, is lower ($1 or 2\mathring{A}$) and the depth of the potential well($E_B = 1 - 2eV$) is greater than the thermal energy.This potential hole depth gives a measure of how strongly the molecule is bonded with the surface. To be desorbed from the surface, the molecule needs to overcome a potential barrier, i.e. some energy needs to be given to it and usually thermal energy is not enough to overcome the potential barrier for chemisorption.

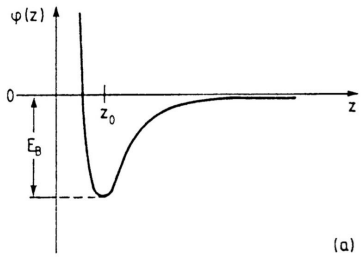

Figure 2: Plot f U(z) for chemisorption

The characteristic quantities of a chemisorption process are:

[1] it may happen that the chemical bonds in the molecule become weaker and so the molecule can be more easily broken

So Q_{diss} represents the energy required to break H_2 molecule in the gas phase, while E_B is the energy required to chemisorb two separated H atoms independently adsorbed on the surface.
Referring to figure 4, when the hydrogen molecule approaches the surface, we can consider two chemisorption paths.

- Path A: the dissociation in gas phase produces two separated H atoms by providing an energy Q_{diss}, then a chemisorption of the 2H atoms occurs at a distance z_c from the surface.
- Path B: first the H2 molecule is physisorbed at distance z_p from the surface. Then there's a transition to dissociative chemisorbed state when the potential barrier E_{act} at z' is overcomed. This potential barrier originates from the superposition of physisorption and chemisorption curves. This energy E_{act} is much lower than Q_{diss}, and at the end the result is the same, i.e. the dissociation into 2H atoms.

To resume, a molecule can be more easily dissociated when adsorbed on a surface, than in gas phase, because the chemisorption process changes the internal electron strucuture of the molecule, reducing its binding energy.

1.2 A2. Concerning the growth process of a thin-film on a surface, explain: - the difference between the three main growth modes of a thin film: Frank–van der Merve (layer by layer), Vollmer–Weber (island growth) and Stranski–Krastanov (layer+islands); - how the growth process can be described in a simplified way using surface tensions; - how it is possible to account for a nonequilibrium pressure.

The growth of a thin film can be of three different types:

- layer by layer, or 2D or Frank-Van Der Merve(FM)
- island growth, or 3D or Vollmer-Weber (VW)
- layer plus island growth or Stranski-Krastanov (SK)

The first mode we see is **layer by layer** or Frank-Van Der Merve. It occurs when the interaction of the adatom with the surface is stronger than the interaction between two near adatoms.
The starting point is the accumulation of nuclei on a surface that tend to grow only laterally [2]. The result is the formation of a single monolayer. This type of growth is typical of epitaxy, where atoms have time to form a good quality layer, but the process is slow.
This process is easier to obtain when the interaction energy between atoms and the surface is stronger than the binding energy of atoms between themselves.

[2] indeed the probability that nuclei accumulates vertically is very low

The different growth modes are related to different values of the contact angle ϕ. In particular:

- For $\phi = 0$ we have a layer by layer growth, where the drop is flat, it only expands horizontally
- For $\phi > 0$ we have an island growth, with a 3D drop

We define an equilibrium condition:

$$\gamma_S = \gamma_{S/F} + \gamma_F cos(\phi) \tag{1.5}$$

From the surface tensions we can predict the contact angle and so the type of growth mode. However γ_S and $\gamma_{S/F}$ are not constant during growth. In fact $\gamma_{S/F}$ changes due to the development of internal stress. And also $\phi = \phi(t)$.
As a consequence, only at equilibrium pressure $p_0(t)$ of the gas phase, we have:

- layer by layer growth for $\phi = 0$, and so $cos\phi = 1$ and $\gamma_S \approx \gamma_{S/F} + \gamma_F$
- island growth for $\phi \approx 90°$, and so $cos\phi << 1$ and $\gamma_S << \gamma_{S/F} + \gamma_F$

Out of the equilibrium pressure [3], we have to consider some corrective parameters. In particular, if $p > p_0(t)$, we are in a condition of supersaturation. Here, we have to take into account the variation of the Gibbs free energy ΔG, produced by N molecules passing from the vapor to the solid phase.

$$\Delta G = n\Delta\mu = Nk_BTln(p/p_0) \tag{1.6}$$

Where the ratio p/p_0 is the degree of supersaturation ratio.
At this point, the equilibrium conditions for the growth modes become:

$$\gamma_S = \gamma_{S/F} + \gamma_F cos\phi - Ck_BTln(p/p_0) \tag{1.7}$$

Thus we have:

- layer by layer growth for $\phi = 0$, and so $cos\phi = 1$ and $\gamma_S \approx \gamma_{S/F} + \gamma_F - Ck_BTln(p/p_0)$
- island growth for $\phi \approx 90°$, and so $cos\phi << 1$ and $\gamma_S << \gamma_{S/F} + \gamma_F - Ck_BTln(p/p_0)$

In high supersaturation ($p >> p_0$) the layer by layer growth is favoured, because the corrective term is negative. This means that the growth mode can be influenced changing the p/p_0 ration, that is an environmental parameter, chosen by us.

1.3 A3. Concerning the energy exchange between a surface and a gas or vapor, explain: - the physical meaning of the accomodation coefficient; - how it can be used to calculate the final temperature of a gas after the interaction with an isothermal surface; - how to calculate the power required to keep constant the temperature of a surface interacting with a constant flow of gas.

The term accomodation coefficient indicates the quality of the energy exchange between the adsorbed atom/molecule and the surface. Indeed the temperature of the gas/vapor may be not the same of the

[3] when sublimation and deposition occur with the same probability, i.e. the solid material is in equilibrium with vapor

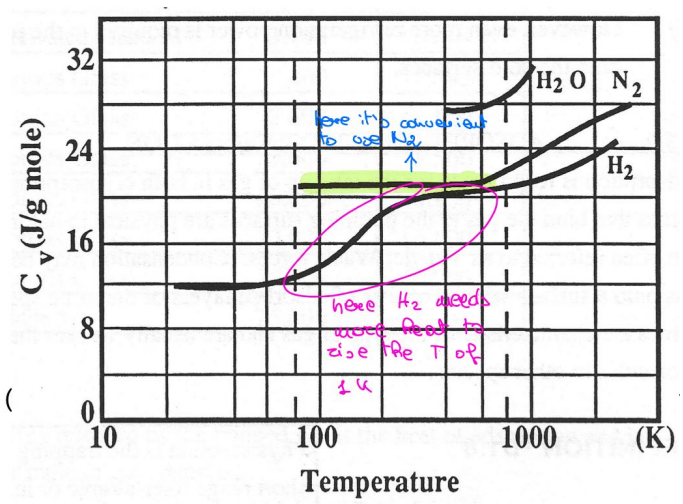

Figure 5: Constant volume molar heat capacity as a function of temperature

If we know how much time is required to change the temperature from T1 to T2, we can calculate the thermal power, i.e. the mean energy which must be given to or removed from the surface per unit time.

$$W = \frac{\Delta E}{\Delta t} = n \cdot c_v \frac{T_2 - T_1}{\Delta t} \tag{1.11}$$

This is the power needed to keep constant the surface temperature during the interaction.
When $W > 0$ the heat is given to the surface, T_g increases $T_2 > T_1$
When $W < 0$ the heat is removed from the surface, T_g reduces $T_2 < T_1$.
Hence, given an initial volume pressure and temperature of a gas, if we know the time interval of the interaction and the final temperature of the gas, we can derive the power needed to keep constant the temperature of the surface. Indeed first we calculate the quantity of gas, i.e. the number of moles, we derive the heat capacity from the graph and at the end we apply the formula for W.
Furthermore, if we know the throughput Q_1, i.e. the flow of gas impinging on a surface, and the temperatures T1 and T2 before and after the interaction with the surface, we can calculate the thermal power as:

$$W = \frac{n}{\Delta t} c_v (T_2 - T_1) = \Phi_{mol} c_v (T_2 - T_1) \tag{1.12}$$

where the molar flow rate is

$$\Phi_{mol} = \frac{n}{\Delta t} = \frac{p_1 V_1}{R \cdot T_1 \Delta t} = \frac{Q_1}{R \cdot T_1} \tag{1.13}$$

At this point we can rewrite the thermal power as:

$$W = \frac{Q_1 \cdot c_v (T_2 - T_1)}{R \cdot T_1} \tag{1.14}$$

that is expressed in Joule as Q1.
Finally, if we are pumping a gas at a pressure p1 and temperature T1, using a cryogenic pump with pumping speed S, then the throughput of the gas flow is:

$$Q_1 = p_1 \cdot S \tag{1.15}$$

If the temperature of the gas is reduced to T2 inside the pump, the power needed to maintain isothermal the pump is:

$$W = p_1 \cdot S_1 \frac{c_v}{R} \frac{T_2 - T_1}{T_1} \qquad [W] \tag{1.16}$$

4

[4] the pressure is expressed in Pa and the pumping speed in $m^3 s^{-1}$

the scattering process.

$$\Gamma = \frac{E_{K(t,1)}}{E_{K(p,0)}} \tag{1.17}$$

It assumes values between 0 and 1. If it is equal to 0 this means that, after the interaction, the target doesn't move, while if it is equal to 1 it means that all the kinetic energy of P has been transferred to T.

In order to define this coefficient as a function of the mass of P and T and the recoil angle, we define some adimensional quantities.

- Ratio between the target and projectile masses $r = \frac{m_t}{m_p} > 0$
- Ratio between the final and initial projectile speed $x = \frac{v_{(p,1)}}{v_{(p,0)}} >= 0$
- Ratio between the final target speed and the initial projectile speed $y = \frac{v_{(t,1)}}{v_{(p,0)}} >= 0$

As a consequence, the energy transfer coefficient can be rewritten as

$$\Gamma = \frac{E_{K(t,1)}}{E_{K(p,0)}} = \frac{m_t v_{(t,1)}^2}{m_p v_{(p,0)}^2} = ry^2 \tag{1.18}$$

If we rewrite y as

$$y = \frac{2cos\phi}{r+1} \tag{1.19}$$

at the end:

$$\Gamma = \frac{4m_p m_t}{(m_p + m_t)^2} cos(\phi)^2 \tag{1.20}$$

If the scattering happens in one dimension, then $\phi = 0$

$$\Gamma = \frac{4m_p m_t}{(m_p + m_t)^2} \tag{1.21}$$

If we average over the all possible angles $\phi \in [0, \pi]$ we get

$$< \Gamma >= \frac{2m_p m_t}{(m_p + m_t)^2} \tag{1.22}$$

1.5 A5. Concerning the process of classical elastic scattering between two particles, explain - the meaning of the scattering constant K; - how it can be expressed as a function of the masses of projectile and target and the scattering angle θ.

Another important parameter in the elastic scattering theory s the **scattering constant K** that measures the energy change of the projectile during the scattering process

$$K = \frac{E_{K(p,1)}}{E_{K(p,0)}} \leq 1 \tag{1.23}$$

Then by exploiting the same adimensional quantities defined in question A4. we can express K as:

$$K = \frac{E_{K(p,1)}}{E_{K(p,0)}} = \frac{m_p v_{(p,1)}^2}{m_p v_{(p,0)}^2} = x^2 \tag{1.24}$$

At the end the speed ratio x can be expressed as:

$$x(r,\theta) = \frac{cos\theta \pm \sqrt{r^2 - sin^2\theta}}{1+r} \tag{1.27}$$

and by multiplying both numerator and denominator by m_p, we get

$$x(m_p, m_r, \theta) = \frac{m_p cos\theta \pm \sqrt{m_t^2 - m_p^2 sin^2\theta}}{m_p + m_t} \tag{1.28}$$

- For $m_t > m_p$
  - only the solution with a plus sign is possible
  - all scattering angles are possible
- For $m_t \leq m_p$
  - both solutions are possible
  - only forward scattering is possible $\theta \leq \pi/2$
  - the scattering angle is limited by the condition $sin\theta \leq r = m_t/m_p$

By squaring the speed ratio, we get the scattering constant as a function of the two masses and the scattering angle.

$$K(m_p, m_t, \theta) = \frac{E_{K(p,1)}}{E_{K(p,0)}} = (\frac{m_p cos\theta \pm \sqrt{m_t^2 - m_p^2 sin^2\theta}}{m_p + m_t})^2 \tag{1.29}$$

From a measure of K, we can get the information about the two masses.

1.6 A6. Concerning the interaction of ions with a surface, explain: - the main characteristics of the sputtering regimes: single knock on, linear cascade and spike; - how the masses of ions and surface atoms influence the efficiency of the sputtering process; - how the surface composition influences the emission of positive and negative ions.

Ions are sent towards a surface to measure and modify some surface properties. Different interaction processes may occur between the ion and the surface which are:
- reflection of the ion
- emission of an electron, called secondary electron
- implantation of the ion that remains inside the material
- collision cascade between the atoms of the surface
- electromagnetic waves emission
- emission of atoms or clusters from the surface as a consequence of the ion impact, sputtering.

This process of removal of atoms from the surface is called **sputtering**. Three regimes of sputtering exist: single knock on regime, linear cascade regime and spike regime.

In the **single knock on regime** the primary ion energy is $E < 1keV$. This kinetic energy of the ion

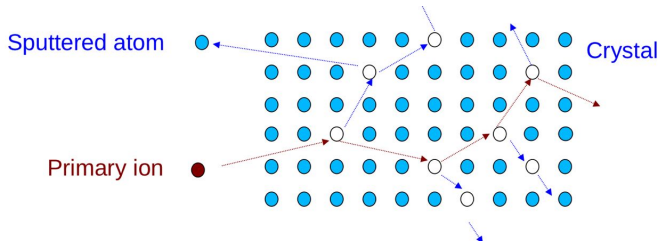

Figure 9: Spike regime

Let's consider the elastic collision between an ion of mass m_I impinging on an atom (target) pf the surface of mass m_A, initially at rest. The energy transfer coefficient measures how much energy is transferred from the ion to the atom: $\Gamma = \frac{E_{K(A,1)}}{E_{K(I,0)}}$ and its average value is $< \Gamma >= 2\frac{m_I m_A}{(m_I+m_A)^2} = \frac{2r}{(1+r)^2}$.

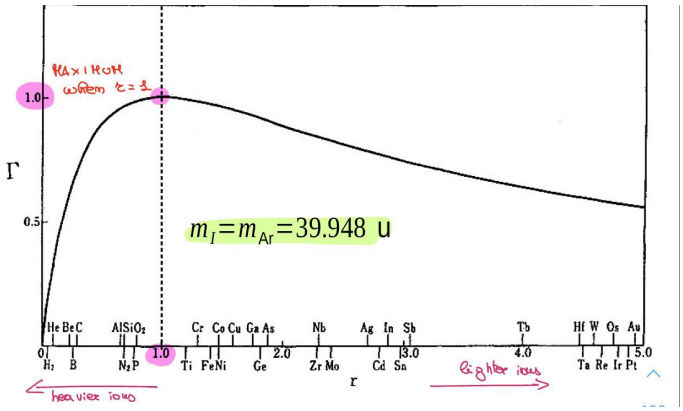

Figure 10: Energy transfer coefficient as a function of the mass ratio r.

From the graph we can notice that in order to have the maximum transfer of energy, i.e. $\Gamma = 1$, we need to use an ion with mass as close as possible to the mass of the atom of the surface.
Moreover, if the ion energy is greater than a certain threshold, usually $E_i > E_0 \approx 4E_s$ (typically 30eV), which depends on the binding energy of surface atoms, the target atom can be emitted from the surface, so sputtering occurs.
In order to get a quantitative description of the efficiency of the sputtering process, we define the **sputtering yield Y** as:

$$Y = \frac{\#\ particles\ extracted\ from\ the\ surface}{\#\ impinging\ ions} \tag{1.30}$$

that for relatively low ion energies($< 1keV$) it is proportional to the ion energy:

$$Y = \frac{3\alpha}{\pi^2}\frac{m_s \cdot m_i}{(m_s+m_i)^2}\frac{E_i}{E_s} \tag{1.31}$$

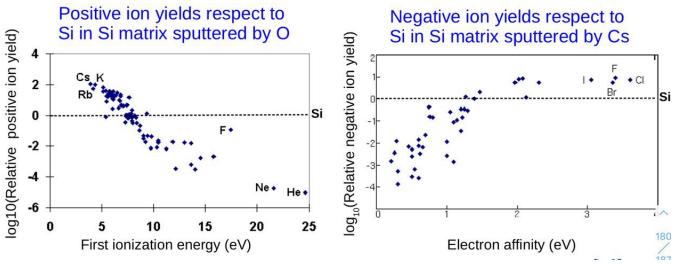

Figure 12: Positive and negative ion yields

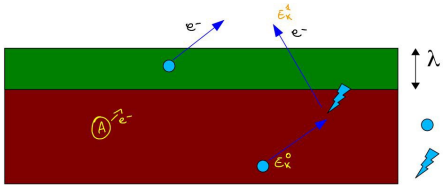

Figure 13: Auger Effect

However, only a fraction of electrons are able to travel from the original atom to the surface without being scattered. And the probability that an electron reach the vacuum outside without being scattered is expressed by the **mean free path**, that is the average length that an electron can travel without scatter.
This parameter depends on the composition of the material, on the electron energy E, on the electron wave vector k and on the crystallographic direction [1]. Actually, the mean free oath in solids is a function of their kinetic energy but is nearly independent from the material, because the major interaction mechanism is the excitation of plasmon waves, whose energy is determined by electron density in the solid.
We can talk also about the **electron escape length** λ, that is the depth under the surface ensuring us that electrons coming from there were not be scattered previously. Typically, it assumes values between $5 \div 20\mathring{A}$.
Electrons coming from a region $< \lambda$ are emitted maintaining their kinetic energy, and they contributes to the formation of peaks in the energy spectrum. On the other hand, electrons emitted at a depth $> \lambda$ are scattered during their path inside the material, and contribute to the background noise of the energy spectrum.

Now, let's see more in detail the Auger process, understanding the physics behind this phenomenon and, in particular, why the Auger electrons emission happens. Indeed the Auger process can be divided in four steps.

1. **Interaction of a primary electron** at energy $2 \div 5keV$, with a core-level electron of an atom.
2. During this interaction, the primary electron releases some energy to the core-electron, a **secondary electron** leaves the core level creating a hole and reaching vacuum. At the end, both primary and secondary electrons leave the surface and the atom is left in a ionized state $A \rightarrow A^+$.

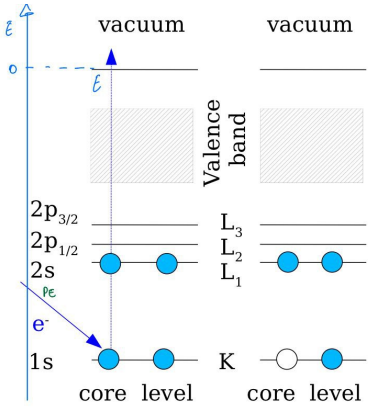

[1] if we deal with a crystalline material

There are two types of **surface sensitivity**, one related to the depth under the surface and one related to the lateral resolution.
Let's consider, for example, an electron beam incident to the surface normally. These primary electrons will excite the electrons of the sample, but only the ones at a depth under the surface $< \lambda$ are not scattered and maintain their original energy. The electron beam has a quite small lateral dimension (3nm), but the electrons collected come from a larger region (100nm), this is due to the fact that primary electrons are scattered and move laterally, exciting also the atoms in the surrounding. The length of the region from which AE are emitted is called **lateral resolution** and it is around 100nm.

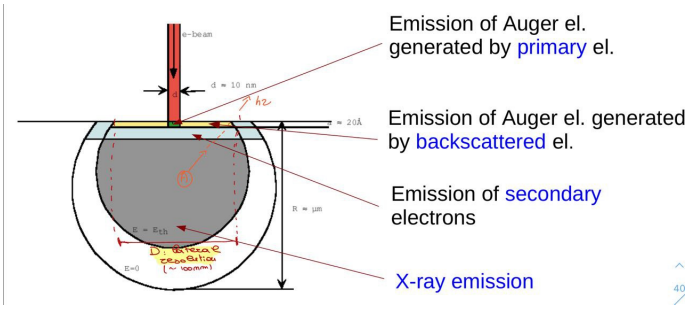

Hence, in other words, the lateral resolution defines the area of the surface from which we get information. The high lateral spatial resolution is one of the main advantages of AES, even if the beam is in principle very narrow. This property allows the acquisition of the chemical maps of the sample, i.e. we can study how the composition of the surface change in different points, by defining some pixels. High resolution, means very small pixels. Every pixel of the map shows an intensity that is proportional to the concentration of a specific element.

As we've anticipated previously, the AES spectrum shows the intensity of the electron detectors signal as a function of the electron kinetic energy. It is a measure of the energy distribution of the Auger electrons collected by the detector. A peak in the spectrum at a given energy E_0, is related to the presence of a particular chemical element on the surface. However, in the spectrum there is also a large background, that is basically noise, due to the collection of secondary electrons at the detector level.

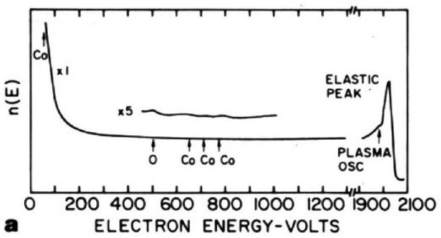

Figure 14: Example of an AES spectrum

It may happen that, like in the figure above, the background completely dominates over the signal, because the Auger emission is not so probable and the intensity of the peaks is small.
In order to reduce the effect of SE background we can perform the same measurements in the **derivative mode**. It allows to detect directly the derivative of the spectrum curves and then enhance the signal-to-noise ratio. This because the background is quite flat and its derivative is null.
In order to directly acquire a physical quantity that is proportional to the derivative of the spectrum, we have to first superimpose a small alternating voltage $v(t) = v_0 sin(\omega t)$ to the outer cylinder DC

From the two graphs we can appreciate that, in the derivative mode, there's a much better separation between the peaks and the background, i.e. the SNR has been improved. Moreover, actually each peak in the integral mode, becomes 2 peak in the derivative mode.

2.2 B2. Describe the X-Ray Photoemission Spectroscopy (XPS) technique, explaining specifically: - the relation between the energy of the photoelectron and the binding energy of the atomic level from which it is emitted, including the role of the work functions of sample and detector; - the origin of the surface sensitivity and the effect of surface charging; - the physical meaning of the chemical shift.

X-ray Photoemission Spectroscopy (XPS), like AES, is a surface sensitive characterization technique belonging to Electron Spectroscopy.
XPS has a better surface sensitivity[2] than AES since it is able to provide stronger signals and for this reason it allows to study also the chemical shift phenomenon.
Moreover XPS can analyze also insulating materials, like AES, even if we need an electron gun to compensate for the surface charge effect.
The goals of XPS are the same of AES, but now the surface is excited in a different way. Indeed, instead of electrons, photons are injected towards the sample and at the end the electrons emitted, resulting from a photoelectric effect, are collected and studied.
The first difference is that the penetration deprth of photons in the material is much longer with respect to electrons, because the interaction between photons and the material is quite weak. Also here, however, we define an escape length λ that is the depth under the surface for which an electron coming from that region is not scattered and maintain its original kinetic energy.
The physic at the basis of XPS is the **photoelectric effect**.
The surface is irradiated by a monochromatic UV (UPS) or X-Ray beam (XPS). In general, depending on the energy of the incoming photon, we get different information. Then the photons are absorbed by the atoms of the material, by releasing their energy to them. This excess energy is able to excite photoelctrons that will escape from the material and are collected in an energy spectrum.
For what regard the incoming photon energy:

- if $E < 50eV$ we are in the UV range and the technique is called UPS
- if $E \approx keV$ we are in the X-ray range and the technique is called XPS or ESCA.

We simplify the photoemission process through a 3-step model:

- optical excitation of an electron from an initial state to a final state within the crystal
- propagation of the excited electron to the surface
- emission of the electron from the surface.

[2] minimum amount of a certain element that the technique is able to recognize

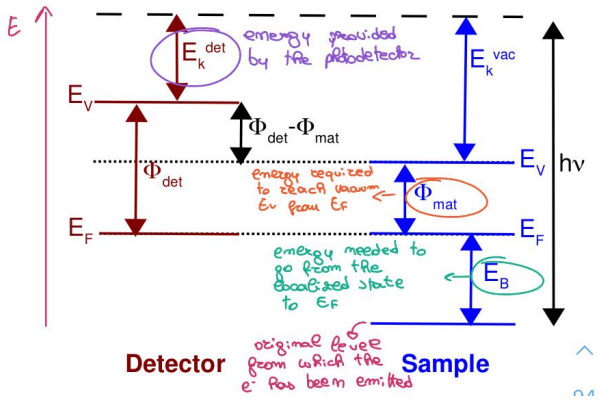

Where the photoelectron energy in the spectrometer is given by:

$$E_k^{det} = E_k^{vac} - (\Phi_{det} - \Phi_{mat}) = h\nu - E_B - \Phi_{mat} - (\Phi_{det} - \Phi_{mat}) = h\nu - E_B - \Phi_{det} \tag{2.10}$$

Using this formula is better because the detector doesn't change, so E_k^{det} is fixed.
If instead the sample is an insulator, we can't do a common ground and when a (neutral) photon impinge on the surface, this will develope a positive charge layer due to the emission of electrons. This positive layer has no effect on photons, but it change the material workfunction, that becomes time dependent. As a result XPS peaks will be shifted

$$E_B = h\nu - E_k - \Phi_{mat} \rightarrow E_B^1 = h\nu - E_k - \Phi_{mat}^1 \tag{2.11}$$

In this case, we have to introduce an electron gun with a beam of low energy electrons that compensate for charge losses.

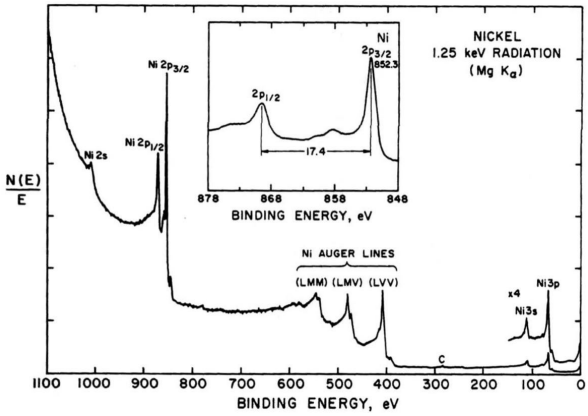

Figure 16: XPS spectrum of Ni irradiated by a X-ray radiation of photon energy 1.25keV

Looking at this spectrum, we can see that there are high intensity peaks due to electrons emitted from Nickel atoms at different core levels, but there are also some small peaks that are due to the emission of some AE. This occurs because after the emission of PE, the atom is left in an ionized state and so it's possible an internal rearrangement that lead to the emission of AE. Again, we confirm that the sensitivity of XPS is greater than the one of AES.

When studying the spectrum, however, we have to take into account another phenomenon, the **chemical shift**. The origin of this effect is that differently bonded atoms, return different binding energies.

SIMS is also the best suited to make depth profile analysis and in this case we deal about "dynamic SIMS". While, when only the compositional analysis of the topmost atomic layer of a sample is performed, we talk about static SIMS.
This is a destructive technique because atoms of the material are extracted from the surface and ionized by means of an ion bombardment, and then analyzed respect to their charge/mass ratio.
The physical basis of this technique is **ion mass spectrometry**, consisting in collecting ions emitted from the surface and in their classification depending on their mass/charge ratio. So, the result is not an energy spectrum like usual, but a mass spectrum.
We are basically sampling directly the surface, by removing matter from the surface and sampling its composition. The result is a more precise technique, but destructive at the same time.
First, an ion beam (primary ions) is focused and accelerated towards the sample. They impact on the sample, extracting (sputtering) atoms, electrons and other ions (secondary ions) from it. We are interested to secondary ions and to analyze by means of a mass spectrometer that is able to filter ions depending on their m/q. At the end, the mass spectrum of SI contains the information about the surface composition of the sample.
The atoms are extracted from the surface by means of a sputtering process and we know that different sputtering regimes may exist, depending on the energy ion beam.
The efficiency of sputtering is measured through the **sputtering yield Y**

$$Y = \frac{number\ of\ particles\ extracted\ from\ the\ material}{number\ of\ impinging\ primary\ ions} \tag{2.12}$$

The primary ion beam instead is characterized by the **primary ion current density**

$$J_{PI} = e\nu \tag{2.13}$$

where e is the electron charge and ν is the ion flux density, i.e. the number of impinging ions per unit area and unit time. Since, we usually deal with single charged ions, if the substrate is conductive, we can measure the current and from it get J.
Another important parameter is the **average lifetime of adsorbates** that is the time that an atom, on average, remains on the surface before being sputtered. If the ion beam intensity is low, this time is high and vice versa. In order to define it, we start from a surface completely covered by an adsorbate layer so that the surface density of adsorbed atoms before sputtering is n_0. Then, the surface density after a time t of sputtering process is $n(t)$. The coverage $\theta(t)$ of the adsorbate layer is defined as the fraction of surface that is covered by the adsorbate layer after a time t of sputtering. The coverage is given by

$$\theta(t) = \frac{n(t)}{n_0} \tag{2.14}$$

If we define the number of impinging ions on an area A of the sample in a time interval dt as
$dN_{ions} = \nu A dt$
and the number of adsorbate particles removed from the surface in a time interval dt as
$dN = -\theta(t) Y dN_{ions} = -\frac{n(t)}{n_0} Y \nu A dt = -\frac{N(t) Y \nu}{n_0} dt$
from the differential equation, we can calculate the number of particles adsorbed on the surface A at a given time t

$$N(t) = N_0 exp(-\frac{Y\nu}{n_0} t) \tag{2.15}$$

Thus, the density of adsorbed particles at time t is

$$n(t) = \frac{N(t)}{A} = n_0 exp(-\frac{Y\nu}{n_0} t) = n_0 exp(-\frac{t}{\tau}) \tag{2.16}$$

Where τ is the average lifetime of adsorbed particles, and it is related to the sputtering efficiency from

$$\tau = \frac{n_0}{Y\nu} = \frac{e n_0}{Y J_{PI}} \tag{2.17}$$

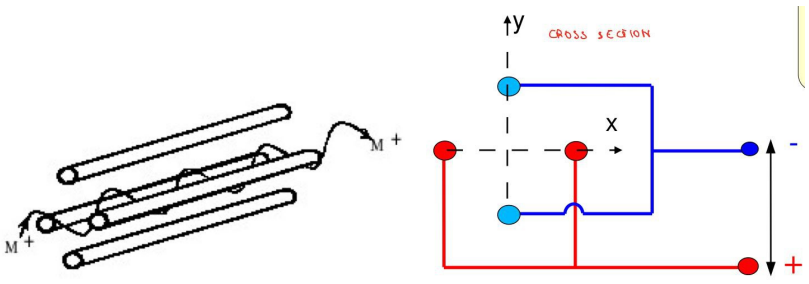

Figure 19: QMS

The rods are equidistant between each other and tha bias is applied in a way that 2 opposite rods have the same potential. So the 2 rods on the x axis are connected to a positive terminal while the 2 rods on the y axis are connected to the negative terminal. Then a potential difference is applied between the two terminals.

$$\Delta V(t) = 2[U_0 + V_0 cos(\omega t)] \tag{2.19}$$

Where U_0 is the static potential and $V(t)$ is the dynamic potential, with $V_0 = 0 \div 1keV$ and $U_0 = V_0/6$.
If we wanna detect another type of ion we have to change V_0 and U_0 maintaining fixed to 6 their ratio.
The ion entering within the 4 bars of the spectrometer is then subjected to an acceleration varying in time and in space in the x-y plane.

$$a_x = -\frac{-2e}{mR_0^2}[U_0 + V_0 cos(\omega t)]x \tag{2.20}$$

$$a_y = +\frac{-2e}{mR_0^2}[U_0 + V_0 cos(\omega t)]y \tag{2.21}$$

Let's consider just the two extreme cases of very high and very low ion masses.
When the mass of the ion is high it is not able to follow the high frequency field and so the effect of $V(t)$ is negligible, and the equations simplify as

$$a_x = -\frac{-2e}{mR_0^2}U_0 x \tag{2.22}$$

$$a_y = +\frac{-2e}{mR_0^2}U_0 y \tag{2.23}$$

By solving the equations of motion we obtain an harmonic oscillation of the ion along the x-direction $x(t) \propto cos(\omega t)$ and an exponential movement along the y-direction $y(t) \propto exp(\omega t)$.
If the rods are long enough, the ion hits one of the rods positioned on the y axis, discharging the ion, that is not able to reach the end of the spectrometer anymore.
On the other and, when the mass of the ion is low, the effect of the time-varying field dominates the motion since $V_0 >> U_0$ and the acceleration components are given by:

$$a_x = -\frac{-2e}{mR_0^2}V_0 cos(\omega t)x \tag{2.24}$$

$$a_y = +\frac{-2e}{mR_0^2}V_0 cos(\omega t)y \tag{2.25}$$

So in the x-direction there's a forced oscillation with the same frequency ω and amplitude increasing with time, while along y-axis the ion has a stable oscillation. This meas that, if the

at the same time and, then, for a time interval, we don't want other ions arriving, otherwise we will have mixed results. We need to wait the time necessary for all the injected ions to arrive. This means that we need a pulsed beam and liquid metal sources are more suitable to make it. With just one pulse we get the whole spectrum, but we have to repeat the analysis to improve the SNR.
ToF spectrometers are suitable for static SIMS analysis, because it's not easy to analyze the strong signals of dynamic SIMS with this technique.

The result of a static SIMS measurement is the **mass spectrum**, which provides the number of ions detected versus their mass. There may be the emission of both single atoms or clusters of atoms. In the second case it may be a problem, because the q/m is not unique, is quite similar for different clusters.

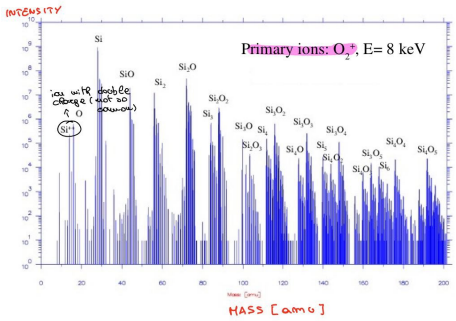

The information given by the detector is the secondary ion current as function of the ion mass

$$I_{SI}(M) = I_{PI} Y \alpha \eta \theta_M \tag{2.31}$$

So it depends on the PI beam intensity, on the sputtering rate and the ionization degree, on the QMA trasmissivity and on the mass coverage.
Typical values of primary ion current density are $j_{PI} = 10^{-9} - 10^{-10} A/cm^2$, with sputtering rate $R = 10^{-4} - 10^{-5} monolayer/s$ and secondary ion current densities $J_{SI} = 10^{-16} A/cm^2$.
The surface sensitivity of static SIMS is higher than AES and XPS, because the SIMS detection limit is 10^{-6} monolayers.
In dynamic SIMS, instead t we measure the depth profile of the concentration of one or more element and we plot it as a function of the sputtering depth. In order to do that, we need much higher sputtering rates with $J_{PI} = 10^{-4} - 10^{-5} A/cm^2$. However, high sputtering rates limit the mass resolution because noise increases and so we have to do a trade off between high sputtering rate and mass sensitivity.

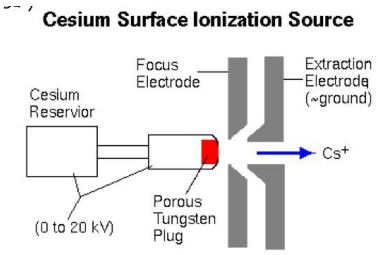

Figure 22: Surface ionization Cs source

Liquid metal ion sources rely on the ionization by field effect of a liquid metal layer covering a tip.
This works only for a limited number of ions. Typically Ga^+ ions, which have a very low evaporation temperature, are evaporated on a sharp tungsten needle, by applying a potential to the tip. Indeed, due to the narrow size of the tip, we have a strong intensification of the field near the tip.
The ion beam intensity is low, so that low sample damage is obtained. Another advantage is that the lateral dimension of the beam is very small (around 10nm) providing a good spatial resolution, useful for chemical maps. Moreover, we can turn ON/OFF the beam, since we can switch ON/OFF the bias applied on the beam, making this kind of source useful for pulsed beams.

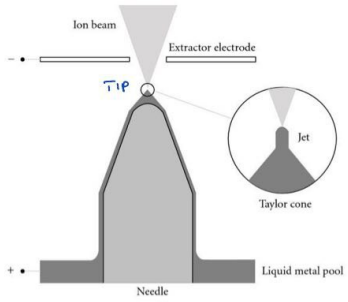

Figure 23: Liquid metal ion source

Once that the ion beam has been created, it is accelerated toward the surface with an energy between 1 and 10keV, and focused through a series of lenses.
In general, for dynamic SIMS higher beam intensity is requested, while for static SIMS lower beam dimension are required to achieve better spatial resolution.

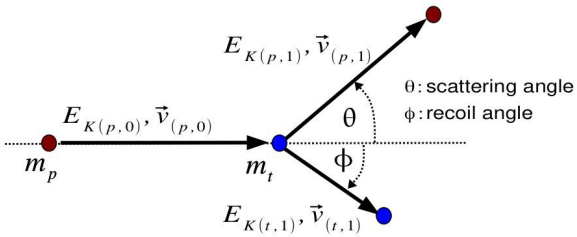

Figure 24: Elastic scattering scheme

The **scattering constant K** is defined as the ratio of the projectile kinetic energies after and before the scattering.

$$K(m_p, m_t, \theta) = \frac{E_{K(p,1)}}{E_{K(p,0)}} = [\frac{m_p cos\theta + \sqrt{m_t^2 - m_p^2 sin\theta^2}}{m_p + m_t}]^2 \qquad < 1 \tag{2.34}$$

Being the scattering angle θ fixed by the position of the detector and the mass m_p by the type of PI beam used, actually the only variable is the mass of the target m_t, so $K(m_t)$.
Thus, we can identify the target ion mass measuring the energy change of the projectile during the scattering process.

In the following graphs we can see how the scattering angle and of the type of primary ion affects the scattering constant curves.

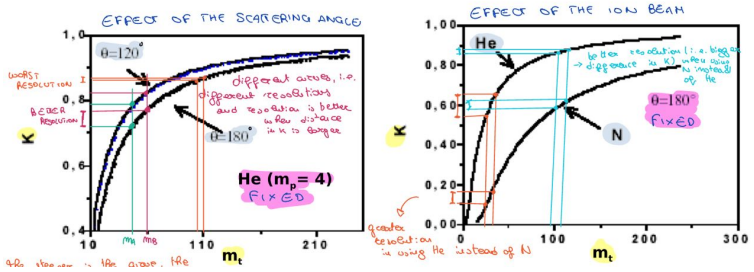

Figure 25: Scattering constant K vs Target mass

For what regard the effect of the angle (left graph), we can see that lighter ions are easier to detect because for such values the curves are steeper and allows us a better resolution (bigger difference between two points on the same curve). Instead, the more flat is the curve, the worst is the resolution. Concerning the effect of the ion beam, we get a greater resolution for heavier targets when N is used, while for lighter targets He ensures higher resolution.

The **RBS** spectra shows the energy distribution of the scattered ions. The energies of scattered ions depend on the scattering constants K of the elements present in the sample.

So, in order to detect light ions like hydrogen, a different scattering configuration is used, the **ERDA**.
It still relies on elastic scattering, but now the impinging ions have greater mass respect to the target. The latter recoils in a forward direction and is extracted from the lattice.
If the angle of incidence is low enough,the target ion can be detected and analysed because the probability of the target scattering (and successive sputtering) is higher when this angle is small.

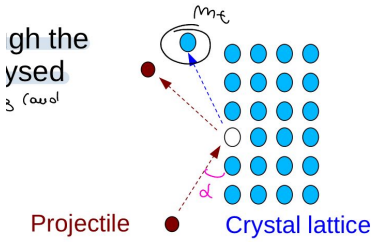

In ERDA the energy distribution of the target ions extracted is analysed, while in RBS we detect the same ions we inject and sputtered.
RBS and ERDA are complementary techniques, the fist is used to detect heavy elements while ERDA is used for the detection of light elements and it is destructive.

2.6 B6. Describe the X-Ray diffractometry (XRD) technique, explaining specifically: - how the X-ray diffraction mechanism can be described using the Laue condition and the Ewald sphere; - how the X-ray diffraction mechanism can be described using the Bragg law; - how the Bragg-Brentano and Thin-Film geometrical configurations work and which type of crystal planes can be observed in the two configurations.

Another bulk sensitive technique is **X-Ray diffractometry (XRD)**, that differently from the previous ones, doesn't require ultra high vacuum conditions.
XRD is mainly used for the structural analysis of the bulk of a material, allowing to :

- identify the crystal structure of the sample
- evaluate the crystallinity fraction of a micro/poly-crystalline material
- evaluate the average size of crystal grains
- evaluate the orientation of crystals

The physical basis of this technique is the **diffraction of X-ray radiation** from a crystal structure. The sample is firstly irradiated by a monochromatic X-ray radiation that impinge with a certain incidence angle. The radiation is, then, diffracted by the crystals in the sample and the intensity of the radiation diffracted by the sample is analyzed at different detection angles. The outcoming radiation is still monochromatic, so we don't have an energy spectrum of photons.

We position the sphere in such a way that the tip of the arrow of the wavevector k in the reciprocal space touches an arbitrary lattice point O of the lattice. It doesn't matter what point, because the reciprocal lattice has a traslational symmetry.The tail of the arrow instead is in the center of the sphere, i.e. C. This construction allows us to identify the direction at which there is constructive interference. Indeed the sphere may touch some points of the reciprocal lattice, like P for example. The vector going from C to P is basically $|\vec{k'}|$, and it satisfies the Laue condition, since the vector G connects connect two points of the lattice, P and O.
Thus, according to figure 29, the condition of constructive interference is achieved only for the values of α that satisfy the Laue condition.

However, there is another way to find this condition, based on the real lattice.

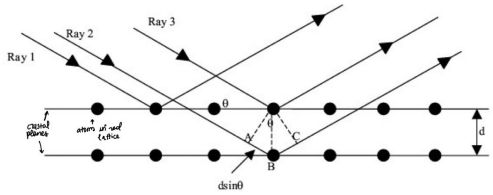

Figure 30: Real lattice

In the above plot, we consider the interference of 2 parallel X-rays reflected by parallel crystallographic planes at a relative distance d.
Now, the condition for constructive interference on the detector, so for having the maximum of intensity, is given by the **Bragg law**. Consider the crystal planes as they are mirrors for the X-rays, the law states that:

$$2dsin\theta = n\lambda \tag{2.36}$$

where θ is the angle of incidence of X-rays respect to the crystal planes, λ is the X-ray wavelength, d is the distance between two crystal planes and n is the order of diffraction.
Moreover, what the law is telling to us is that the angle at which the ray is detected respect to the crystal plane, must be equal to the angle of incidence, always respect to the crystal plane.

The XRD equipment consists of three main parts: an X-ray emission tube, a monochromator and a X-ray detector, and the experimental setup is shown in the following.

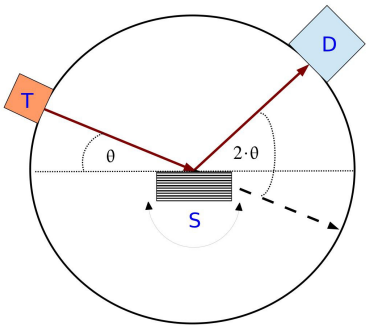

Figure 31: XRD experimental setup

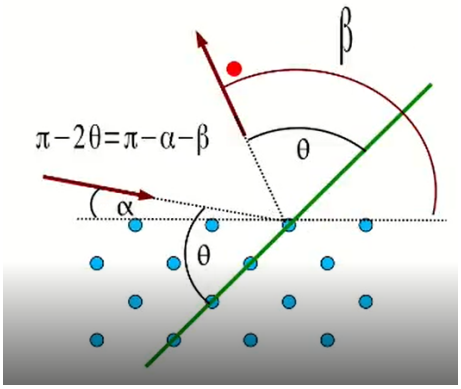

Figure 34: TF configuration

Referring to figure **??**, for such value of β, we get that the incidence angle with respect to the crystal plane (θ) is equal to the detection angle with respect to the crystal plane (θ). And the value of θ can be recovered easily from α and β as:

$$\alpha + \beta = 2\theta \tag{2.37}$$

In the BB configuration all the sample volume contributes to diffraction, while in the TF configuration, since the angle of incidence is very small, the penetration depth of X-ray is very small and the depth of material contributing to the signal is given by just:

$$d = \lambda sin(\alpha) \tag{2.38}$$

For this reason we talk about thin film, even if d is not of the order of nm like in surface sensitive characterization techniques, it is several microns or hundreds of nanometers.

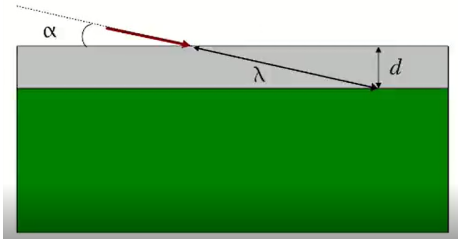

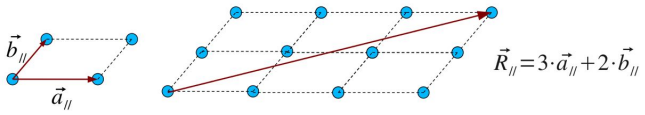

When considering a 2D lattice, we can define the surface reciprocal lattice, starting from the base vectors:

$$\vec{a^*_{//}} = 2\pi \frac{\vec{b_{//}} \times \hat{n}}{|\vec{a_{//}} \times \vec{b_{//}}|} \tag{2.42}$$

$$\vec{b^*_{//}} = 2\pi \frac{\hat{n} \times \vec{a_{//}}}{|\vec{a_{//}} \times \vec{b_{//}}|} \tag{2.43}$$

With $\hat{n}$ the unit vector normal to the surface.
From these we can define the translation vector in the reciprocal space as

$$\vec{G_{//}} = n\vec{a^*_{//}} + m\vec{b^*_{//}} \qquad with\ n, m\ integers \tag{2.44}$$

It can be shown that the **condition for constructive interference** is:

$$\vec{k'_{//}} - \vec{k_{//}} = \vec{G_{//}} \tag{2.45}$$

This condition is similar to the Laue condition already seen in XRD for diffraction by 3D crystals, but here we can have much more possibilities of constructive interference with respect to volume diffraction. We can say that in surface scattering we have a relaxation of the third Laue condition.

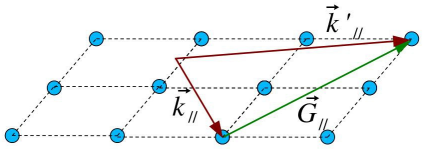

Due to this relaxation, in **2D diffraction** we have many more values of k' and k that give rise to constructive interference, w.r.t. the 3D case. Also here, we show geometrically the interference condition using the Ewald sphere, drawing a set of rods in the z direction, starting from the points of the reciprocal lattice. The constructive interference condition is satisfied every time that sphere and rods intercept.
Thus, overall, we say that we observe more diffraction peaks in surface diffraction compared to bulk one because 2D diffraction involves only the components parallel to surface of wavevectors.

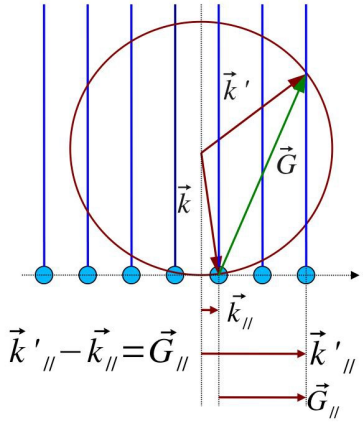

However, a simple inspection of the geometry of the diffraction patterns allows to get useful information about the surface structure. Indeed, for a good quality surface, with regular arrangement of atoms and low density of defects, we have a regular LEED pattern with well-defined spots. While the presence of surface defects broadens the spots and increases the background noise.
LEED is particularly useful for studying the long-range order and periodicity of surfaces. By analyzing the diffraction pattern, researchers can deduce the lattice parameters, symmetry, and surface reconstructions of the material.

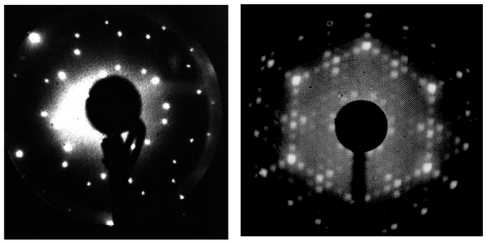

Figure 36: (left)LEED pattern taken on the surface of Pt crystal in the 111 direction. Sharp spots identify points of the surface reciprocal lattice. (right) LEED pattern taken on Si 111 surface with 7x7 reconstruction. It is very noisy because it is a 3D structure

On the other hand, in the **RHEED experimental setup**, high energy electrons (10-100keV) impinge on the surface with a very low incidence angle. Since the energy is higher, such electrons are able to penetrate deeper in the material, but a good surface sensitivity is still get due to the low angle of incidence. Indeed, higher energy means shorter wavelengths, allowing for more precise investigations.
Also in this case, the result is the generation of a diffraction pattern on the screen, even if different w.r.t. the LEED one.
The RHEED technique is especially useful for in situ analysis of surfaces that have been modified previously.

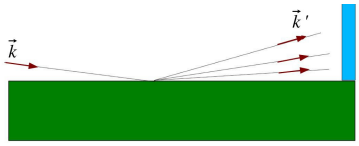

Figure 37: RHEED setup

Due to the high electrons kinetic energy, the radius of the Ewald sphere (equal to $|k| \propto \sqrt{E}$) is much longer than the spacing between the rods of the reciprocal surface lattice.

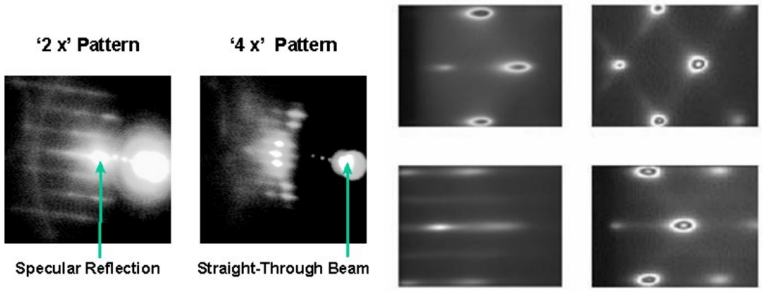

Figure 39: (left) RHEED patterns taken on the surface of a GaAs sample during MBE growth. Diffraction lines proofs the smoothness of the film surface. (right) RHEED patterns taken during different stages of MBE growth

Both LEED and RHEED are non-destructive techniques that provide valuable insights into the atomic structure and dynamics of surfaces. They are widely used in materials science, surface physics, and nanotechnology research to investigate the properties of thin films, crystal surfaces, and interfaces

Let's see now the main differences between the equipment of the two techniques.
In the LEED case, we start with an electron gun whose energy is between 20 and 500eV. Then, we need some electron optics in order to collimate the electron beam. There are also some retarding grids, biased with a negative potential w.r.t. the surface. This produces an electric field that slows down the electrons, in order to suppress the background due to electrons that were subject to inelastic scattering. The result of this electric field is the formation of a potential barrier that electron can overcome only if they have high enough energy But, in this case, the energy is very small, so we need also accelerating grids, i.e. grids with opposite bias to accelerate electrons. At the end, a fluorescent screen and a data acquisition system are needed.

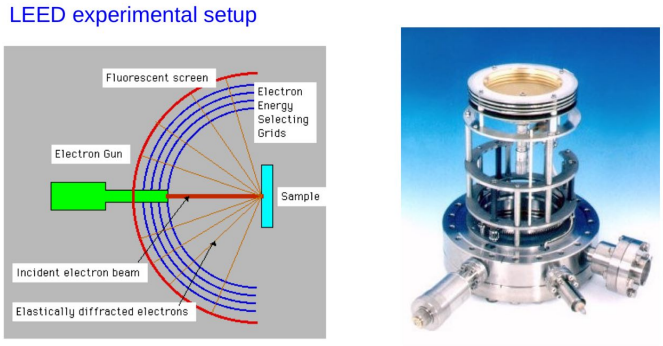

Figure 40: LEED experimental setup

For the RHEED process, instead, we need an electron gun whose energy is between 10 and 100keV, electron optics for collimation of the electron beam, a fluorescent screen and a data acquisition system. Hence, no grids are required, because elastically scattered electrons have enough energy to produce fluorescence on the screen, while ineleastically scattered not.

atom. Such interference results into a fine structure in the X-ray absorption spectrum, that can be seen only with a high resolution detector.

Moving to a more quantitative analysis, we can describe the intensity of radiation absorbed with an exponential decay law.

$$I(x) = I_0 e^{-\mu \cdot x} \tag{2.46}$$

With x the depth under the material surface, I_0 the X-ray intensity at the surface and $I(x)$ the X-ray intensity at depth x. While μ is the absorption coefficient and it is a function of the material and of the photon energy $\mu = \mu(h \cdot \nu)$. If the beam is monochromatic, the absorption coefficient will change depending on the wavelength of the radiation. In the X-ray range μ decreases more or less monotonically for increasing energy, except at the absorption edges, where ionization occur.

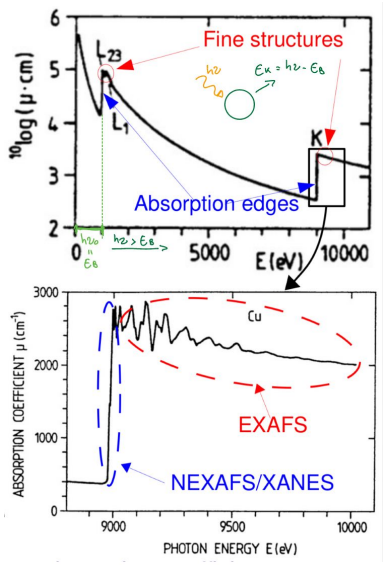

Figure 42: Absorption coefficient versus photon energy (Cu sample)

At each absorption edge, the photon energy reaches the minimum value needed to produce ionization from a certain atomic shell, which means that from the position of the absorption edge we can extract the information about the binding energies of the electron shells in the atom.

Whereas the high energy side of the edge is characterized by an oscillatory fine structure (circled in red). Such oscillating behaviour of μ can be analyzed in detail in the bottom figure of 42. The EXAFS analysis (i.e. information on the atomic bonds) is based on the interpretation of these fine structures. The oscillations arise due to the scattering of the ejected photoelectron by neighboring atoms in the material. The wavefunction of the scattered photoelectron interfere with the incident X-ray wave, resulting in constructive and destructive interference patterns that are manifested as the fine structure in the absorption spectrum.

EXAFS and NEXAFS are characterized by different probability of scattering since, as we said before, their photon energy ranges are distinct: up to $\approx 1keV$ after the edge for the EXAFS and up to $\approx 50eV$ after the edge for the NEXAFS.

If the X-ray photon energy is near an absorption edge, the photoelectron emitted from the atom has a very low kinetic energy, meaning that while leaving the atom, the photoelectron interacts with the chemical environment (first neighbours). As a result, such neighbours can act as scattering centers for the photoelectron wavefunction. On the other hand, in the fine structures there's lower probability of scattering, thus we can neglect the possibility of multiple scattering events.

- measure the intensity I_0 of the X-ray beam imipinging on the sample
- measure the intensity I_T of the X-ray beam transmitted by the sample
- know the sample thickness d

$$\mu = \frac{1}{d} \cdot log(\frac{I_0}{I_T}) \quad [7] \tag{2.50}$$

EXAFS is a bulk sensitive technique, since the beam travels across the whole sample volume before being detected and atoms absorbed on the surface give only a negligible contribution to the final signal.

To extract information about the first atomic layers of the sample we need to refer to the **SEXAFS** technique. In order to enhance the surface sensitivity, the absorption coefficient μ is measured in an indirect way. Instead of measuring the ratio between the transmitted radiation and the X-ray beam intensity, in SEXAFS we evaluate the number of Auger electrons emitted by the surface for a given X-ray excitation energy. The probability of Auger emission is fixed and doesn't change with photon energy. Since the Auger electrons have a very short escape length, the surface sensitivity is obtained.

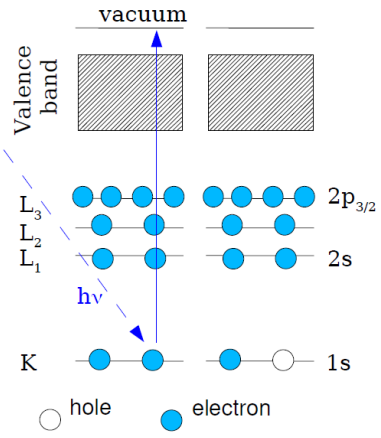

An X-ray photon is absorbed in the core level (K) of an atom, producing the emission of a photoelectron that leaves a hole in that level. The absorption coefficient is proportional to the probability of creation of that hole.

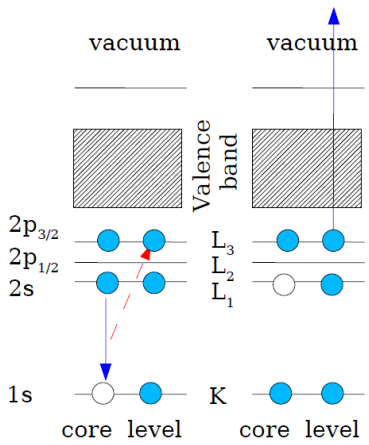

[7] basically, this is the inverse formula of eq.2.46 assuming x=d

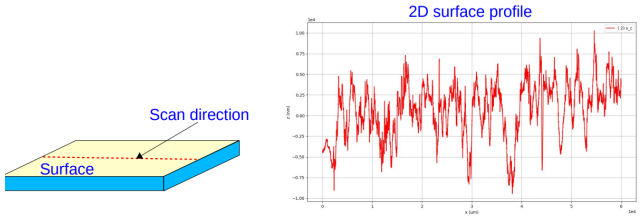

Figure 45: 2D surface profile z vs x

Looking at the figure, the final profile is a set $\{z_i\}$ of values of the variable height z, coupled to the x-values $\{x_i\}$ where $x_i = x_0 + i \cdot \Delta x$. This is a digitalized profile of a continuous function $z = z(x)$, representing the surface section, with:

- scan length $L = N \cdot \Delta x$, where N is the number of acquisition points
- average height or centre line, as the average of the function z(x) over the $[x_1, x_N]$ interval

$$\bar{z} = \frac{1}{L} \int_{x_0}^{x_N} z(x) dx \tag{2.52}$$

that in digitalized form becomes the average of all the evaluated points

$$\bar{z} = \frac{1}{N} \sum_{1}^{N} z_i \tag{2.53}$$

Such $\bar{z}$ is not used for any important information, but it is essential to define a reference for several parameters.

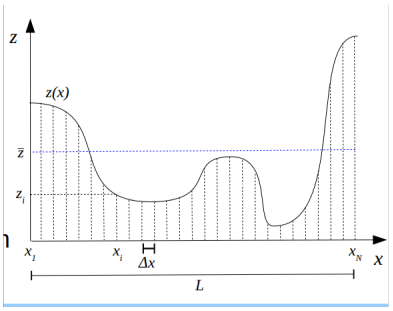

Figure 46: Continuous 2D surface profile z(x)

From the profile of fig.45 we can extract the height distribution compared with a normal distribution with the same parameters.

Another important parameter is the **root mean square deviation** from the centre line R_q or RMS. This is the standard deviation of the height distribution.

- For a continuous profile $R_q = \sqrt{\frac{1}{L}\int_{x_0}^{x_N}[z(x)-\bar{z}]^2 dx}$, which is the square root of the sum of the squares of distances from the mean line
- For the digitalized profile $R_q = \sqrt{\frac{1}{N}\sum_1^N (z_i - \bar{z})^2}$

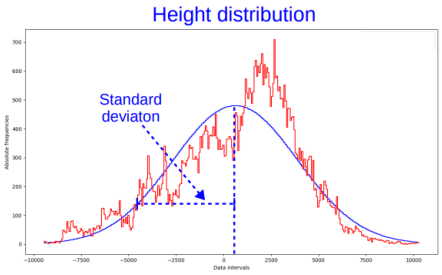

Figure 50: Height distribution, standard deviation

R_q is always greater than R_a: $R_q > R_a$. And, for a normal distribution of heights (i.e. a gaussian), their ratio is

$$\frac{R_q}{R_a} = \sqrt{\frac{\pi}{2}} \approx 1,253 \tag{2.54}$$

Such parameter, w.r.t. before, is more sensible to the presence of high peaks or low valleys.

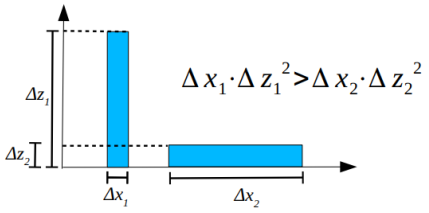

Quite often the surface profile is a superposition of features of **different length scales** and to individuate them, we have to separate the effect of different features into different signals. For example, in the figure three signals with different length scales are superposed. We can see that there's a bigger main undulation, small undulation along it and some spikes, which occur all at different scale.

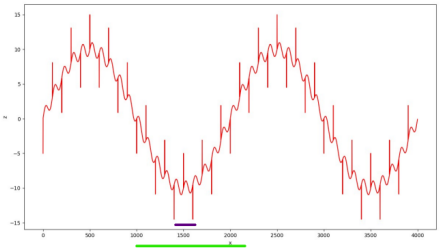

Figure 51: Roughness/Waviness separation. In violet is highlighted the small scale, in green the big scale

2.10 B10. Concerning the analysis of the surface roughness of a material, explain: - the definition and meaning of the Rku (kurtosis) and Rsk (skewness) parameters; - how it is possible to separate the information related to the surface morphology at different scale lengths.

For the introductory part about surface roughness, see question B9

From the surface profile and from its height distribution, other two parameters can be derived.

The first one is the **skewness** of the profile R_{sk}. It describes the form of the distribution in terms of symmetry or asymmetry of data. In particular, it indicates whether the distribution tail is moved left or right relative to the center of the distribution.

- On the continuous profile, $R_{sk} = \frac{\frac{1}{L}\int_{x_0}^{x_N}[z(x)-\bar{z}]^3 dx}{R_q^3}$ or equivalently $R_{sk} = \frac{1}{L}\int_{x_0}^{x_N}\left[\frac{z(x)-\bar{z}}{R_q}\right]^3 dx$
- On the digitalized profile, $R_{sk} = \frac{\frac{1}{N}\sum_1^N (z_i-\bar{z})^3}{R_q^3}$ (i.e. the ratio between the average of the cube of distance points from the mean line and the cube of R_q) or equivalently $R_{sk} = \frac{1}{N}\sum_1^N \left(\frac{z_i-\bar{z}}{R_q}\right)^3$. This time it matters wether the point z_i is above or below the mean line (+ or - contribution).

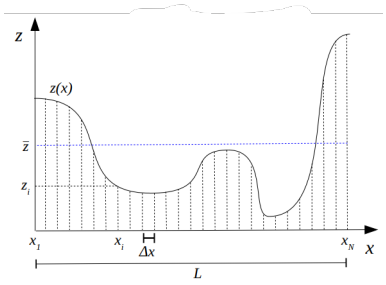

Figure 54: 2D surface profile z(x)

For a normal distribution $R_{sk} = 0$

- if $R_{sk} < 0$ the mean value is negatively shifted respect to the peak
- if $R_{sk} > 0$ the mean value is positively shifted respect to the peak

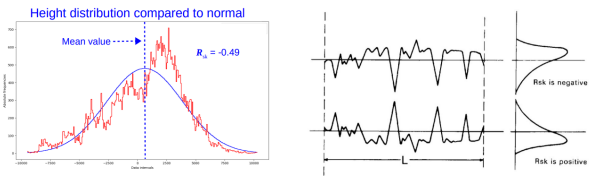

Figure 55: Heigh distribution, skewness

The other parameter is the **kurtosis** of the profile R_{ku} (the fourth moment). Starting from the plot of the continuous profile z(x) as a function of x, it is defined as:

THERANOSTIC NANOMATERIALS

4.1 What are the key parameters in a nanoparticle affecting its interaction with biological fluids?

One smart approach to do theranostic could be by exploiting Nanotechnology, and in this case, we often use the term Nanomedicine. Indeed, the use of nanoparticle (NP) or nanosized platforms allows to do therapy or an imaging action, which then becomes a diagnosis of the patient disease. A Nanomedicine becomes theranostic when it combines, in one single nanoparticles tool, both therapeutic and diagnostic actions.
The first reason why a nanoparticle can interact with biological fluids is that both NP and cells have more or less the same size. Specifically, among cells and molecules we deal with dimensions between 1nm and few μm[1], which are comparable with NP extension.

- mm (10^{-3} m): organs, tissues giant cells
- µm (10^{-6} m): cells and organels
- nm (10^{-9} m): ultrastructure of cell organels

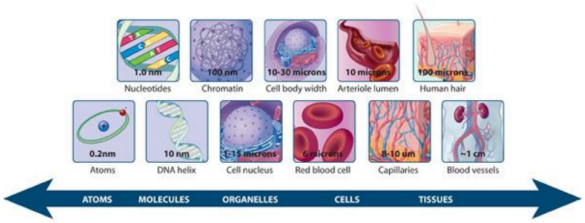

Figure 58: Measure units of cells and organels

When in contact with a biological fluid, the nanomaterial properties have to match with the ones of the biological world.

In particular, the nanomaterial is created at the laboratory level by a group of physicist, chemists and nanoscientists, and the characteristics to be tailored are: size, shape, chemical functionality, surface charge and surface and material composition.

Whereas, biology sets the requirements of the specific nanobject. For instance, we have to know which kind of signaling and biomarker has a certain cancer, at which kinetics the tumor mass grows, and which kind of transportation mechanism the NP has to adopt to reach it. Moreover, each tumor

[1] bacteria cells are $1\mu m$ large

- decreased dosing frequency;
- reduced rate of rise of drug concentration in blood;
- sustained and consistent blood level within the therapeutic window, i.e. within the minimum threshold for therapeutic efficacy and the physiological toxic level;
- enhanced bioavailability, i.e. reducing the metabolization of the drug;
- achieve targeted drug release;
- reduced side effects;
- improved patient compliance.

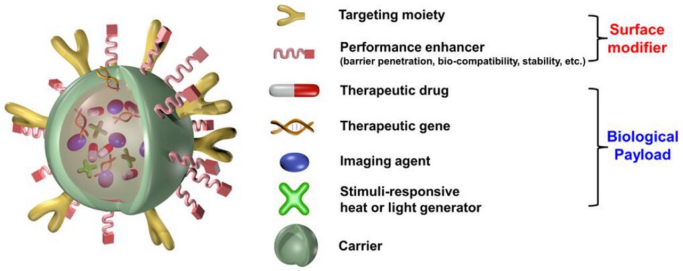

Figure 60: Theranostic Nanoparticle Design

Let's see the design of a theranostic nanoparticle. Its main components are the carrier (the particle itself), the surface modifier and the biological payload.

The carrier can be both organic or inorganic based. It must provide sufficient physical protection for its content under physiological conditions during delivery to the target site.

For what regard the surface modifier, attached to the surface of the carrier, it regards all the elements able to interact with the biological environment of the body.

- The *targeting moiety* that contains the address of the final destination of the NP, i.e. where the drug has to be delivered.
- The *performance enhancer*, that can be either a biological, organic or polymeric molecule whose role is to help the NP to travel throughout the biological system and to penetrate the physiological barrier of the target tissue. For example, when dealing with a brain tumor, we have to know that the brain is a quite impenetrable natural barrier called "blood brain barrier" (BBB), so only very specific enhancers can pass through it.

Concerning, instead, the internal biological payload, it is devoted to the modification of the biological function of the target cell, and it is made up of:

- The *therapeutic drug* is the drug itself, like: anticancer drugs, DNA, small interfering RNA (siRNA), proteins, hyperthermia-inducing nanoparticles, ROS-generating agents, and so on.
- The *therapeutic gene* needs to modify the genetic content of the cell.
- The *imaging agent* is used to visualize the disease and, so, to permit a diagnosis. It can be an organic dye, a quantum dot, upconversion particles, MRI or CT contrast agents, and so on.
- The *stimuli-responsive heat or light generator*, which, more in general, has a specific way (not necessarily by heating or light emission) to trigger a specific action of the NP, that can be, for example, the release of the therapeutic agent inside the cell.

3 antibodies, that once they link with the receptors, allow the internalizatino of the NP inside the cancer cell, with consequent drug delivery.

In the EPR (passive) case instead, the NP arrives first into the blood vessel and only in correspondance of some specific fenestrations, originated by the presence of a growing tumor mass, it can pass and arrive to the site of interest.

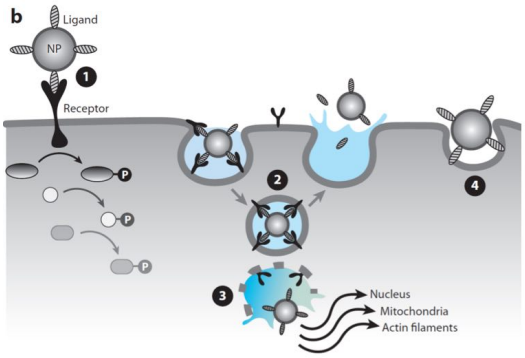

Figure 62: Targeting ligands, in-vitro studies

There are four different possibilities of interaction between the ligand and the receptor.

1. The ligand-receptor bond catalyzes, without entering the cell, a cascade of biochemical signaling inside the cell which can lead to the cell death or, at least, to the interruption of its proliferation. Actually, immunotherapy works in a similar way. Instead of the whole NP, you inject just a monoclonal antibody that binds with the receptor of the cancer cell, leading to cascade signaling. In this context, using a NP is preferable since it can be exploited as imaging too and, in general, it preserves the ligand.

2. The ligand-coated nanoparticles can also be internalized and exocytosed by the cell, without ever leaving the vesicle, by first bind to the receptor, enter the cell and then exit from it. The created vesicle is called endosome.

3. After have been internalized into the cell, it may happen that the NP damages the endosome membrane, escapes from the vesicle and interact with various organelles present in the cell citosol, like nucleus, mitochondria and active filaments.

4. The NP ligands don't interact with the receptors of the cell, but the internalization is still possible due to the fact that the cancer cell is very hungry. The drawbacks is that suche interaction is far more slower (24h vs 2/5h of previous methods) and not specific.

Another factor that is important to mention is the surface density of the targeting ligands on the NP surface and the receptor density on the cancer cell. Once such moieties bind with the biomarkers, the lipid raft effect occurs. This is a reorganization of the lipidic bilayer due to the release in the Gibbs free energy, which induces the cell membrane to wrap around the NP to form a closed-vesicle structure: the endosome. The result is that the receptors are now closer.

4.4 In the design of a theranostic nanoparticle, which are the possible roles of a carrier?

The carrier is one of the three main component of a theranostic nanoparticle, together with the (internal) biological payload and the (external) surface modifier. The carrier constitutes itself the

- **Therapeutic functions**: delivering the payload to the target site (i.e. drug delivery) or being a therapeutic agent itself. For example, a metal (like Au) NP, if excited by NIR light, spontaneously generates heat, and so it performs a hyperthermic approach that burns the cancer cell. Once the light is turned off, the action of gold nanomaterials ceases.

We have just said that the carrier per se can behave as therapeutic agent. This is possible because the NP responds to a stimuli of energetic nature, like light, magnetic field or pH, activating the therapeutic action only at the exact time and place.

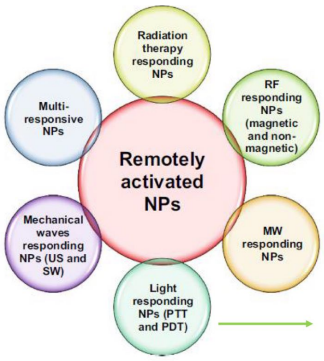

Figure 65: Stimuli-responsive NPs

Then, the carrier is bonded with imaging or therapeutic payloads by means of physical bonds like hydrogen or Van Der Waals forces or through chemical conjugations like electrostatic, covalent bonds or $\pi - \pi$ interaction. According to the type of bonding, also the release kinetics of the drug.

Between the carrier and the payload can be established specific biologically-labile bonds of different nature. They can be: biological, physical or chemical, or combination of them. Each one has a specific triggering mechanism for the activation of the therapeutic action.

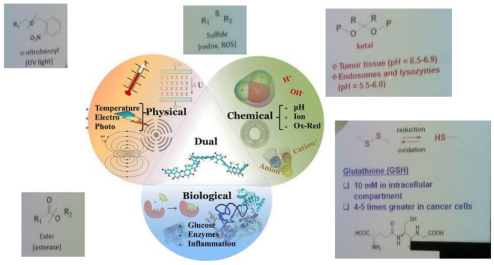

Figure 66: biologically-labile bonds

Furthermore, it's important to modify the surface of the carrier in order to define how the nanomaterial will behave in the biological fluid.

In conclusion, the most important requirement of a nanocarrier is **safety**. The carrier has to safely deliver the imaging or therapeutic payload to the tumor site in a target-specific manner, preferably through the adoption of triggerable bonds. Obviously, safety means also protection of the payload under physiological condition and also no release in unwanted time and space.

Hence, the requirements that the theragnostic NP has to fulfill in order to ensure safety are:

1. Removal from the body of conventional drugs via urinal excretion or liver metabolic pathways.

- Hetero-aggregation, where the medium is further "complicated" by the presence of some proteins. Here, we can see the formation of the protein corona that neutralizes the particle and leads to aggregation and, then, precipitation.
- Dissolution, when inserted into a biological system of ions and proteins, the NP starts to chemically degrade itself dissolving slowly into ions and other pieces of material. So, at the end, the particle doesn't exist anymore.

In conclusion, engineers have to ensure NP stability into the biological fluid, and a possible solution to rapid clearance and NP aggregation is to coat the surface of nanomaterials with a poly(ethylene)glycol (PEG) layer. This prevents opsonization, i.e. the creation of opsonin proteins in the protein corona. The opsonin is unwwanted since it attracts the mononuclear phagocyte system (MPS), basically the macrophages, that recognize the NP as an external particle and clear it out to the spleen and liver. Instead, with the presence of a PEG layer, the opsonin formation is blocked and the blood half-life of the nanomaterial is drastically increased.

Such PEG layer can be linear or branched, and engineers have to tailor its thickness and density.

Another important factor affecting the NP behaviour in blood is the size.

- Nanoparticles with diameter $<$ 6nm, even with the PEG layer, are excreted by the kidneys, due to the fact that the kidney pores are larger than 6nm, and are quicly eriminated from the body.
- Nanoparticles with diameter

  $>$

  200nm accumulate in the spleen and liver, where they are processed by macrophages.
- $6nm < NP\ diameter < 200nm$ is the optimal size, since it allows the permeation in the pores of the blood vessels and the accumulation in the tumor mass, by means of the EPR effect. However, if the NP is made of toxic elements, like QDs made of CdSe or it carries a chemotherapeutic drug, it accumulates in the liver and the spleen leading to some problems.
- The best choice is to exploit nanoparticles made of degradable materials like polymer, lipids or hydrogels. In this way the degradation is time-controlled, the NP can circulate in a stable way into the biological media and, only after 1 or 2 weeks, it is degradated into safe bioproducts.

4.6 What is the EPR effect and why is it important when developing theranostic nanomaterials?

The EPR (Enhanced Permeation and Retention) effect is a phenomenon observed in tumor tissues that allows certain nanoparticles to accumulate preferentially in tumors rather than into healthy tissues. This effect arises due to the unique characteristics of tumor blood vessels and the impaired lymphatic drainage commonly found in solid tumors. Indeed, cancer cells are really hungry cells and create (angiogenic) blood vessel network where they tend to attract oxygen and nutrients in order to proliferate as much as possible.

Tumor blood vessels are often poorly formed, leaky, and irregularly shaped, with fenestrations (50 to 200nm) between the cells that make up the vessel walls. This means that NPs with size lower than 100nm can travel in the bloodstream and once they arrive to the blood vessels, they can attach directly to the tumor mass. This is a totally passive process from the NP point of view.

Additionally, tumor tissues lack functional lymphatic vessels, which normally help drain fluids and particles from the tissues. As a result, nanoparticles can passively extravasate from the blood vessels into the tumor interstitium, but they have difficulty exiting the tumor due to the absence of a